

# RSC Advances



This is an *Accepted Manuscript*, which has been through the Royal Society of Chemistry peer review process and has been accepted for publication.

*Accepted Manuscripts* are published online shortly after acceptance, before technical editing, formatting and proof reading. Using this free service, authors can make their results available to the community, in citable form, before we publish the edited article. This *Accepted Manuscript* will be replaced by the edited, formatted and paginated article as soon as this is available.

You can find more information about *Accepted Manuscripts* in the [Information for Authors](#).

Please note that technical editing may introduce minor changes to the text and/or graphics, which may alter content. The journal's standard [Terms & Conditions](#) and the [Ethical guidelines](#) still apply. In no event shall the Royal Society of Chemistry be held responsible for any errors or omissions in this *Accepted Manuscript* or any consequences arising from the use of any information it contains.



Journal Name

ARTICLE

## Perfluoropolyether/poly(ethylene glycol) triblock copolymers with controllable self-assembly behaviour for highly efficient anti-bacterial materials

Received 00th January 20xx,  
Accepted 00th January 20xx

DOI: 10.1039/x0xx00000x

www.rsc.org/

Jing Song,<sup>a</sup> Qun Ye,<sup>a</sup> Wang Ting Lee,<sup>a,b</sup> Xiaobai Wang,<sup>a</sup> Tao He,<sup>a</sup> Kwok Wei Shah,<sup>a</sup> Jianwei Xu<sup>\*,a,b</sup>

A series of perfluoropolyether/poly(ethylene glycol) (PFPE/PEG) triblock copolymers PEG/PFPE/PEG (**P1-P3**) and PFPE/PEG/PFPE (**P4-P5**) were prepared *via* thiol-ene click reaction in high yields. Their chemical structures, molecular weights and thermal stability were characterized by <sup>1</sup>H nuclear magnetic resonance (NMR) spectroscopy, gel permeation chromatography (GPC) and thermogravimetric analysis (TGA), respectively. The spin coated polymer films were characterized in terms of scanning electron microscopy (SEM), atomic force microscopy (AFM) and contact angle goniometer. The polymer **P1-P4** showed wrinkle-like surface morphology at film state, but **P5** exhibited segregated morphology due to its poor solubility in the casting solvent. Polymers **P1-P4** at thin film state displayed high hydrophilicity with water contact angles in the range of 10.2–12.3° and surface energy of 52.7–55.2 mN/m even though hydrophobic PFPE segments were present in the polymer backbone. The anti-bacterial properties of the spin-coated films (**P1-P3**) were tested against *E. coli* and *S. aureus* on Si surface and remarkable anti-bacterial properties were observed for this series of polymers, particularly for **P3** that almost completely prohibits the growth of *E. coli* and *S. aureus*, rendering this type of PEG/PFPE/PEG triblock polymers as high performance antimicrobial coating materials.

### Introduction

Both fluoropolymers and poly(ethylene glycol) (PEG) are among the most widely explored functional polymers for biofouling-release coating materials<sup>1–6</sup> which have wide applications for marine anti-fouling coating and anti-bacterial biomedical device. Fluoropolymers are active to repel bio-organisms mainly due to their low surface energy and a low Young's modulus.<sup>7–9</sup> PEG based materials are well known for their ability to inhibit protein as well as cell adsorption because of the electrostatic repulsion and a hydration effect at the interface.<sup>10–15</sup> Due to good water solubility of PEG, a rational design strategy to prepare robust anti-biofouling material, is to chemically combine PEG and low surface energy fluoropolymers, which would render an intriguing class of amphiphilic materials with potent controllable self-assembly behavior. This strategy has been explored by Wooley,<sup>16–22</sup> Ober,<sup>23–31</sup> and DeSimone.<sup>9, 32–36</sup> Wooley and DeSimone mainly focused on fluoropolymer-PEG co-network polymers for fouling release coating. Ober also demonstrated side-chain block copolymers consisting of grafted ethoxylated fluoroalkyl chains that were able to release both sporelings of *Ulva* and *diatoms*. Despite that

fluoropolymer-PEG based materials have previously been reported, the self-assembly behavior of these amphiphilic materials has seldom been investigated in detail. Furthermore, how an amphiphilic material assembles and how its morphology of the coated material correlates to the anti-fouling or anti-bacterial properties need be addressed. A thorough investigation of these issues would provide more insights for the better understanding and further development of anti-fouling and anti-bacterial materials.

Herein we report a new strategy to prepare perfluoropolyether (PFPE) and PEG based nonfouling coating materials. We adopted a highly efficient thiol-ene click chemical strategy<sup>37–41</sup> to covalently link PFPE and PEG together to synthesize a series of triblock copolymers. Amphiphilic block copolymers<sup>42</sup> are a rather intriguing class of materials due to their controllable molecular weight, well-defined molecular geometry and self-assembly behavior.<sup>43–49</sup> PFPE-PEG triblock copolymers have been reported to prepare water-in-fluorocarbon emulsions<sup>50–52</sup> which can serve as efficient delivery system for T-cells.<sup>53</sup> This novel class of materials, however, has not been studied as nonfouling coating materials despite the great potential. In our current study, we synthesized a series of A-B-A (**P1-P3**) and B-A-B (**P4-P5**) type triblock copolymers with different molecular weights based on PFPE and PEG. The spin coated thin films exhibited an interesting wrinkle-like morphology as revealed by scanning electron microscopy (SEM). It was unexpected that the polymer thin films were more hydrophilic than neat PEG polymer even though hydrophobic PFPE fragments were present in the polymer backbone. The anti-fouling properties of this batch of

<sup>a</sup>Institute of Materials Research and Engineering, A\*STAR (Agency for Science, Technology and Research), 3 Research Link, Singapore 117602.  
Email: jw-xu@imre.a-star.edu.sg

<sup>b</sup>Department of Chemistry, National University of Singapore, 3 Science Drive 3, Singapore 117543.

<sup>†</sup>Electronic Supplementary Information (ESI) available: GPC chromatographs, NMR spectra, calculation of polymer purity. See DOI: 10.1039/x0xx00000x

triblock copolymers were tested against common pathogens *E. coli* and *S. aureus* on Si surface. Remarkably strong anti-fouling properties of **P3** were observed, hence rendering PFPE/PEG based triblock copolymers as a promising class of nonfouling coating materials.

## Experimental

### General

<sup>1</sup>H nuclear magnetic resonance (NMR) spectra were recorded on a Bruker DRX 400 MHz spectrometer in CDCl<sub>3</sub> at room temperature. Spectrometer operating frequency was at 400.13 MHz (<sup>1</sup>H). Tetramethylsilane was used as an internal standard for <sup>1</sup>H spectra. Thermal analysis was performed in a Perkin-Elmer thermogravimetric analyzer (TGA 7) in nitrogen at a heating rate of 20 °C/min. Molecular weights were determined using Waters Model 2690 Gel Permeation Chromatography (GPC) in HPLC-grade tetrahydrofuran (THF) against PMMA as standard. Scanning electron microscope (JEOL LVSEM 6360LA) was used for observation thin film surface morphology. A Bruker Dimension Icon™ atomic force microscope was used for AFM imaging. A contact angle goniometer, model 100-00, (Ramé-Hart, Inc. USA) was used for the determination of static water contact angles. The reported angle was the average of five measurements on different area of each sample. The surface free energy parameters were calculated according to the references.<sup>54, 55</sup> Dynamic light scattering (DLS) measurements were performed with a Bruker device equipped with a HeNe 633 nm laser and a scattering angle of 90°. Fluorescent spectra were recorded using a Shimadzu spectrophotometer (RF-5301PC).

### Materials

3-Aminopropyltriethoxysilane, poly(methyl vinyl ether-alt-maleic anhydride), pyrene, LB broth (10g of tryptone, 5g of yeast extract, and 10g of NaCl), toluene, THF, ethanol, and allyl bromide were purchased from Sigma-Aldrich. 2,2'-((Oxybis(1,1,2,2-tetrafluoroethane-2,1-diyl))bis(oxy))bis(2,2-difluoroethanol) (**1**) and perfluoropolyether diol Z-DOL (**3**) (M<sub>n</sub>: 2500, PDI<1.1) were purchased from Matrix Scientific and Solvay Solexis, Inc., respectively. 2,2-Difluoro-2-(1,1,2,2-tetrafluoro-2-(1,1,2,2-tetrafluoro-2-(trifluoromethoxy)ethoxy)ethoxy)ethanol (**5**) and perfluoropolyether mono-alcohols (**7**) (M<sub>n</sub>: 3745, PDI<1.1) were bought from Exfluor Research Corp. and Daikin Industries, Ltd., respectively. PEG-monothiol (M<sub>n</sub>: 1000) were bought from Nanocs Inc. PEG-dithiol (M<sub>n</sub>: 1000 or 2000) was purchased from Aldrich. All other chemicals for preparation of polymers were purchased from commercial vendors without any further purification.

### Synthesis

Compounds 6,6,8,8,9,9,11,11,12,12,14,14-dodecafluoro-4,7,10,13,16-pentaaxanonadeca-1,18-diene (**2**) and 1,1,1,3,3,4,4,6,6,7,7,9,9-tridecafluoro-2,5,8,11-tetraoxatetradec-13-ene (**6**) were synthesized according to a reported method.<sup>56</sup> Bis-allyl terminated Z-DOL (**4**) and mono-allyl terminated perfluoropolyether (**8**) were synthesized using a similar method (Scheme 1). Commercial perfluoropolyether alcohol (**3** or **7**) (1.984 mmol **1** or 0.982 mmol **3**) was transferred into a 100 mL two-necked round

bottom flask. Sodium hydroxide (20.0 mL, 6.875 mol/L) was added, followed by phase transfer catalyst Aliquot 336® and then the reaction mixture was allowed to react at 40 °C for 2 h. After 2 h, allyl bromide (7.0 mL, 41.33 mmol) was added and the reaction mixture was maintained at 40 °C for a further 6 h. Fluorinated solvent FC77® (10.0 mL) was used to extract the product, followed by washing with deionized water (40.0 mL, 5 times) to remove excess allyl bromide. The FC77® layer was washed again with chloroform (20.0 mL, 2 times) to remove phase transfer agent Aliquot 336®. The FC77® layer was evaporated and the remaining oil was dried by vacuum in an oven at room temperature overnight. Compound (**4**): Yield (92%). <sup>1</sup>H NMR (CDCl<sub>3</sub>, 400 MHz): δ = 5.89-5.81 (m), 5.32-5.23 (m), 4.13-4.11 (d, J = 5.6 Hz), 3.82-3.77 (t, J = 9.6 Hz). Compound (**8**): Yield (94%). <sup>1</sup>H NMR (CDCl<sub>3</sub>, 400 MHz): δ = 5.88-5.81 (m), 5.33-5.23 (m), 4.13-4.12 (d, J = 5.6 Hz), 3.82-3.78 (t, J = 9.6 Hz).

### Synthesis of polymers P1-P3

The A-B-A conformation triblock copolymers (**P1-P3**) were synthesized using bifunctional perfluoro-precursor and poly(ethylene glycol) thiol, *via* a thiol-ene click reaction. Bifunctional perfluoro-precursor **2** or **4** (0.3110 g, 0.1244 mmol) and poly(ethylene glycol) mono-thiol (0.2490 mmol) (M<sub>n</sub>: 1000) were weighed into a 25 mL three necked round bottom flask. Distilled THF (10.0 mL) was injected *via* septum and the system was purged with argon gas for 30 min. Azobisisobutyronitrile (AIBN) (0.0010 g, 0.006707 mmol) was added into the system and then purged for an additional 15 min. Reaction was left to reflux at 80 °C overnight. After cooling down to room temperature, the solvent was removed by rotary evaporation and the residue was dissolved in minimal amount of chloroform and dropped into hexane. The dissolved sticky precipitate was collected and dried by vacuum.

**P1**: Yield (95%). <sup>1</sup>H NMR (CDCl<sub>3</sub>, 400 MHz): δ (ppm) = 3.74-3.71 (m), 3.60 (s), 3.56-3.53 (m), 3.37 (s), 2.92-2.86 (m). GPC: calculated 2490 g/mol, M<sub>n</sub> = 2250 g/mol, M<sub>w</sub> = 2613 g/mol, PDI = 1.16.

**P2**: Yield (93%). <sup>1</sup>H NMR (CDCl<sub>3</sub>, 400 MHz): δ (ppm) = 3.74-3.70 (m), 3.64 (s), 3.55-3.53 (m), 3.37 (s), 2.89-2.86 (m). GPC: calculated 4580 g/mol, M<sub>n</sub> = 4100 g/mol, M<sub>w</sub> = 4470 g/mol, PDI = 1.09.

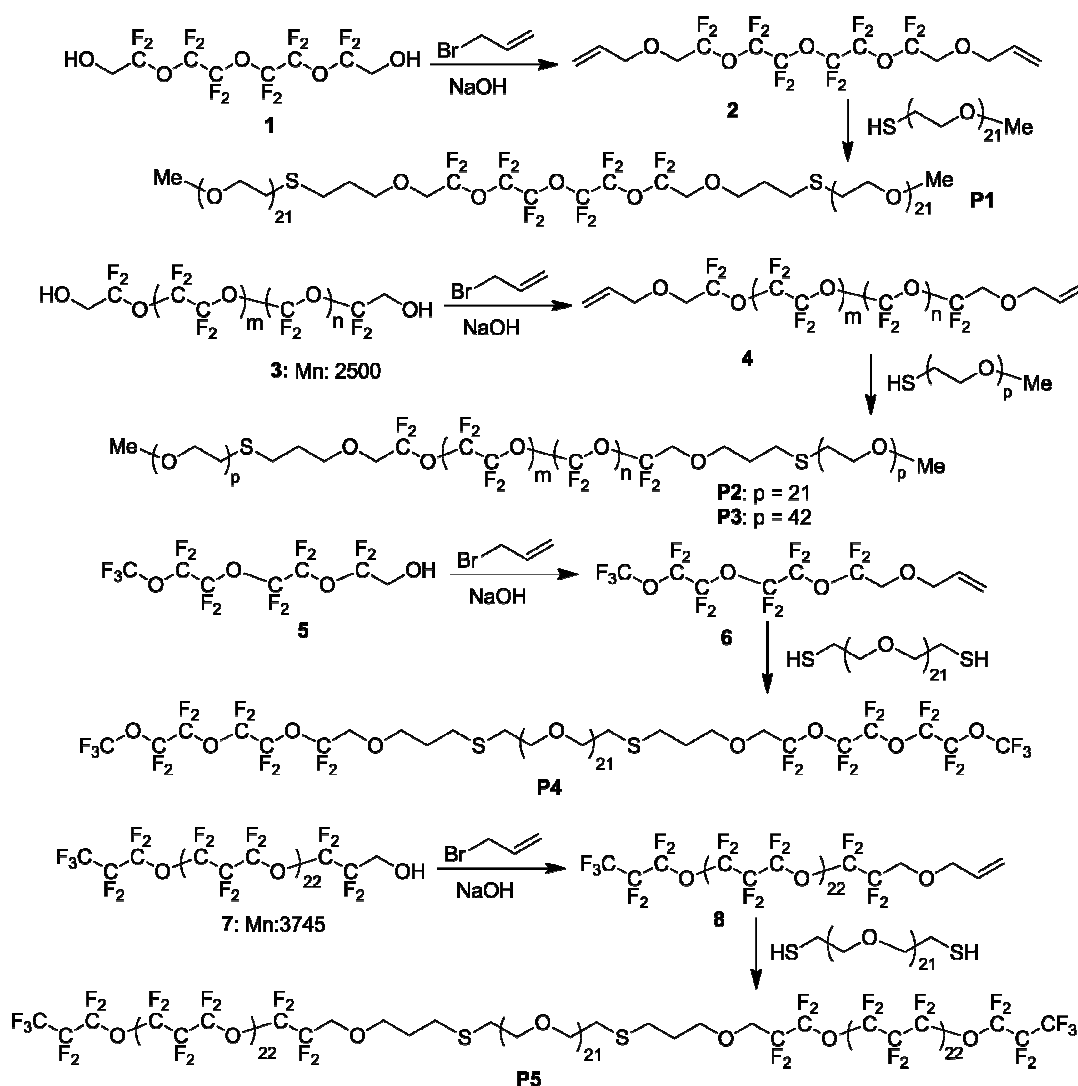
**P3**: Yield (90%). <sup>1</sup>H NMR (CDCl<sub>3</sub>, 400 MHz): δ (ppm) = 3.74-3.70 (m), 3.64 (s), 3.55-3.53 (m), 3.37 (s), 2.89-2.86 (m). GPC: calculated 6580 g/mol, M<sub>n</sub> = 6181 g/mol, M<sub>w</sub> = 6914 g/mol, PDI = 1.12.

### Synthesis of P4 and P5

The B-A-B conformation triblock copolymers (**P4-P5**) were synthesized using monofunctional precursor **6**, or **8**—and poly(ethylene glycol) dithiol, *via* a thiol-ene click reaction. Monofunctional precursor **6** or **8** (0.2 mmol) and poly(ethylene glycol) dithiol (0.1 mmol) were weighed into a 25 mL three necked round bottom flask. Distilled THF (10.0 mL) was injected *via* septum and the system was purged with argon gas for 30 min. AIBN (0.0010 g, 0.006707 mmol) was added into the system and then purged for an additional 15 min. Reaction was left to reflux at 80 °C overnight. For **P4**, after cooling down to room temperature, the solvent was removed by rotary evaporation and the residue was dissolved in minimal amount of chloroform and dropped into hexane. The undissolved sticky precipitate was collected and dried by vacuum. For **P5**, after cooling down to room temperature, the solvent was removed by rotary evaporation and the residue was dissolved by

10ml of FC 77<sup>®</sup>. The FC77<sup>®</sup> solution was extracted with water and the fluorinated portion was collected and dried by vacuum.

solvent. Cloudy suspensions are put into an ultrasonic bath at room temperature for 1 min in order to dissolve the polymer as much as



**Scheme 1.** Synthesis of triblock copolymers **P1-P5**.

**P4:** Yield (96%) <sup>1</sup>H NMR (CDCl<sub>3</sub>, 400 MHz): δ (ppm) = 3.83-3.80 (m), 3.74-3.71 (m), 3.64 (s), 3.56-3.54 (m), 3.38 (s), 2.90-2.86 (m). GPC: calculated 1876 g/mol, M<sub>n</sub> = 1774 g/mol, M<sub>w</sub> = 1920 g/mol, PDI = 1.08.

**P5:** Yield (88%) <sup>1</sup>H NMR (CDCl<sub>3</sub>, 400 MHz): δ (ppm) = 3.75-3.71 (m), 3.65 (s), 2.90-2.86 (m), 2.03 (s), 1.25 (m). GPC: calculated 8570 g/mol, M<sub>n</sub> = 7849 g/mol, M<sub>w</sub> = 9110 g/mol, PDI = 1.16.

#### Solubility Test

The solubility test of **P1-P5** was purely qualitative, based on the appearance of the polymer in various common solvents. Approximately 10.0 mg of polymer was dissolved in 1.0 mL of

possible. Solubility was estimated by cloudiness of the resultant solution relative to the clear solvent. A clear solution is marked as soluble, and cloudy solution is marked as poorly soluble, whereas solubility smaller than 0.1mg/mL is marked as very poorly soluble.

#### Polymer thin film preparation

Polymer thin films for surface characterization were prepared by spin coating a 10% (w/v) chloroform solution of the series triblock copolymers on silicon using a G3P-8 model spin coater (SCS, UK) at 2000 rpm for 30 seconds.

Polymer surfaces (**P1-P3**) for antibacterial assay were prepared on 1 cm × 1 cm silicon substrate. The silicon substrates were cleaned in piranha solution (Sulphuric acid: hydrogen peroxide = 7:3 v/v)

followed by rinsing with deionized water and drying with N<sub>2</sub>. The Si substrates were then soaked in the toluene solution containing 1% (w/v) of 3-aminopropyltriethoxysilane for 4h, and then rinsed with ethanol and dried with N<sub>2</sub>. The above treated substrates were immersed in a THF solution of poly(methyl vinyl ether-alt-maleic anhydride) 1% (w/v) under nitrogen environment for 4h. The substrates were removed from the solution, rinsed rigorously with THF and dried with nitrogen. All the substrates were further spin coated with polymer solutions to prepare the thin film. After casting the thin film, all the samples were baked at 150 °C for 2h in vacuum.

### Antibacterial test

To study the bacterial attachment of *Escherichia coli* and *Staphylococcus aureus* on uncoated and polymer coated Si surfaces, the surfaces were incubated with bacterial containing broth solution and then examined using SEM.

*Escherichia coli* (*E. coli*, ATCC#: 53868) and *Staphylococcus aureus* (*S. aureus*, ATCC#: 25923) were obtained from American Type Culture Collection, ATCC (USA). The bacterial strains were cultured in LB broth (10 g of tryptone, 5 g of yeast extract, and 10 g of NaCl) at 37 °C for about 16h before harvest. The bacteria-containing broth was centrifuged at 3000 rpm for 10 min, and after the removal of the supernatant, the cells were washed twice and re-suspended with phosphate-buffered saline (PBS, pH = 7.4).

After incubation with bacterial suspension for 1h, the samples were washed three times with PBS before fixing with 3% glutaraldehyde for 5h at 4 °C. After the fixation, substrates were rinsed with DI water to remove the remaining glutaraldehyde and then dried at 60 °C in the oven for 24h. The dried samples were coated with gold and then imaged with a SEM.

## Results and Discussion

### Synthesis

The synthetic routes of the PEG (A) – PFPE (B) triblock copolymers are shown in Scheme 1. The A-B-A triblock copolymers were synthesized from PFPE polymers **1** with two hydroxy terminal groups. The terminal OH groups were first converted to allyl group and then the thiol-ene click reaction was applied to link thiol terminated PEG polymers to the two terminal sides of the PFPE polymer. Similar to the preparation of A-B-A type triblock copolymers, the end OH group of PFPE polymer **3** was first converted to allyl group, followed by adopting the same thiol-ene

click reaction to connect two PFPE polymers to a thiol terminated

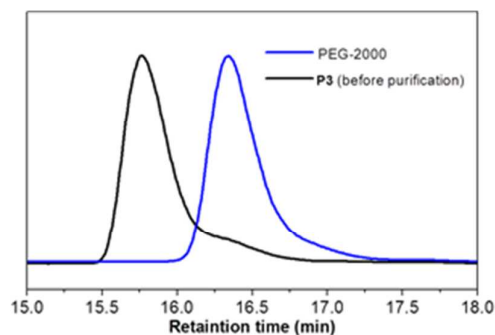


**Figure 1.** Normalized GPC curves of starting material PEG-2000 and polymer **P3** before purification.

PEG polymer. PEG and PFPE polymers with different molecular weights were used and five polymers (**P1-P5**) were prepared accordingly. The triblock polymer compositions, synthetic yields, purity, molecular weights and thermal properties of **P1-P5** are summarized in Table 1. All polymers **P1-P5** were obtained in good yields by thiol-ene click reaction (> 88%) and they showed moderate thermal stability with degradation temperatures in the range of 236–284 °C (obtained from TGA experiments). The purity of polymers **P1-P5** was estimated by using <sup>1</sup>H NMR spectroscopy and the details were included in the supporting information. Polymers **P1-P4** showed very good purity of 94–98%, but the purity of polymer **P5** was relatively low (ca. 90%) probably due to low reactivity of mono-allyl-substituted perfluoropolyether (**8**) with large molecular weight. The experimental molecular weights of polymers **P1-P5** with relatively low PDI in the range of 1.08–1.16 were in good agreement with the theoretical values.

The thiol-ene click approach could be monitored by GPC analysis with polymer **P3** as an example shown in Figure 1. The starting polymer PEG-2000 had a retention time at 16.3 minutes and this peak gradually depleted during the thiol-ene click reaction process and a new peak with a retention time at 15.8 minutes appeared. After the reaction was finished, the peak corresponding to the starting polymer almost diminished and the triblock polymer **P3** was fully formed.

The solubility of polymers **P1-P5** was examined in various solvents and the results are summarized in Table 2. For polymers **P1**, **P2** and

**Table 1.** Composition, molecular weight, yield and thermal property of **P1 - P5**.

Polymers	Conformation	PEG (A) Mw	PFPE (B) Mw	Calc. Mw <sup>a</sup>	Expt. M <sub>n</sub> <sup>b</sup>	PDI <sup>c</sup>	Yield (%)	Purity (%) <sup>d</sup>	T <sub>d</sub> (°C) <sup>e</sup>
<b>P1</b>		ca 1000	490	2490	2250	1.16	95.0	95.0	284
<b>P2</b>	A-B-A	ca 1000	ca 2580	4580	4100	1.09	93.0	97.4	244
<b>P3</b>		ca 2000	ca 2580	6580	6181	1.12	90.0	94.5	270
<b>P4</b>	B-A-B	ca 1000	438	1876	1774	1.08	97.0	97.6	254
<b>P5</b>		ca 1000	ca 3785	8570	7849	1.16	88.0	90.2	236

<sup>a</sup>: Calculated molecular weight; <sup>b</sup>: Experimental number-average molecular weight from GPC; <sup>c</sup>: polydispersity index (PDI); <sup>d</sup>: polymer purity was estimated by <sup>1</sup>H NMR spectroscopy (Supporting Information); <sup>e</sup>: thermal decomposition temperature (T<sub>d</sub>) is defined as the temperature at which 5% weight loss occurs.



**P4**, due to the relatively low molecular weights, these three

**Table 2.** Summary of the solubility of polymers **P1 - P5**

Solvent	P1	P2	P3	P4	P5
Water	√	√	-	√	--
Ethanol	√	√	-	√	--
Acetone	√	√	√	√	-
Chloroform	√	√	√	√	-
THF	√	√	-	√	-
Hexane	--	--	-	--	-
FC-77 <sup>®</sup>	--	--	-	--	√

√ soluble or dispersed well; -, poor; --, very poor)

polymers were soluble in water and polar organic solvents (ethanol, THF, chloroform, acetone). In comparison with **P1-P2**, polymer **P3** has limited solubility in water, ethanol and THF because of its higher molecular weight, but good solubility in chloroform and acetone due to its higher PEG content. For **P5**, it is only soluble in fluorinated solvents, for example, FC-77<sup>®</sup>, mainly owing to its very high fluorine content as well as high molecular weight.

#### Surface morphology

The amphiphilic triblock copolymer can self-assemble into micelles, fiber, etc. depending on the molecular structure and self-assembly environment in order to minimize energetically unfavourable block-block selective solvent interactions.<sup>57, 58</sup> In chloroform solution, the PFPE/PEG copolymer was envisaged to self-assemble into core-shell bilayer spherical micelles as proposed by Platzman et al.<sup>53</sup> In this work, in order to study the properties of micelle, dynamic light scattering (DLS) measurements were performed. The particle sizes and the critical micelle concentration (cmc) data are summarized in Table 3. All the results were obtained from aqueous solutions.

**Table 3.** Micelle size and cmc characterization

Polymer	Size (nm)	cmc (mg/ml)
<b>P1:</b> PEG <sub>1000</sub> -PFPE <sub>400</sub> -PEG <sub>1000</sub>	100.5 ± 74.2	0.014
<b>P2:</b> PEG <sub>1000</sub> -PFPE <sub>2500</sub> -PEG <sub>1000</sub>	174.0 ± 117.2	0.012
<b>P3:</b> PEG <sub>2000</sub> -PFPE <sub>2500</sub> -PEG <sub>2000</sub>	209.9 ± 120.6	0.011
<b>P4:</b> PFPE <sub>400</sub> -PEG <sub>1000</sub> -PFPE <sub>400</sub>	241.8 ± 173.6	0.010
<b>P5:</b> PFPE <sub>3745</sub> -PEG <sub>1000</sub> -PFPE <sub>3745</sub>	255.5 ± 117.3	0.101

The self-assembled micelle sizes of **P1-P5** were in the range of 100-260 nm with broad particle size distributions. For A-B-A type polymers **P1-P3** and B-A-B type polymers **P4-P5**, the results suggested that the average particle sizes increase with the increase of polymer molecular weights. This is in fact consistent with theoretical study of surfactant micelles.<sup>59, 60</sup> The morphology of spin coated polymer dispersions in chloroform was imaged by AFM. In Figure 2a, isolated sphere particles were observed when diluted **P1** dispersion was used (0.5 mg/ml). When the dispersion concentration increased to 2 mg/ml, the typical AFM image of spin coated surface was displayed in Figure 2b. It can be distinctly seen that the block copolymer **P1** formed isolated but elongated

structure with a diameter around 30-100 nm. The copolymer particles anisotropically aggregated and assembled into elongated structure with the collapse of PEG shell.

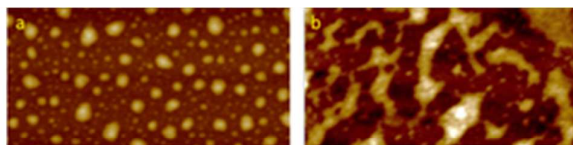


**Figure 2.** AFM images of **P1** self-assembled micelles as prepared by spin coating of their diluted dispersions in chloroform. a) 0.5 mg/ml; b) 2 mg/ml, scan size: 0.5×1μm, z = 20 nm

The surface morphologies of copolymer films were also investigated by SEM in a large area. Figure 3 shows the surface morphology of **P1** dispersion as prepared by spin coating.

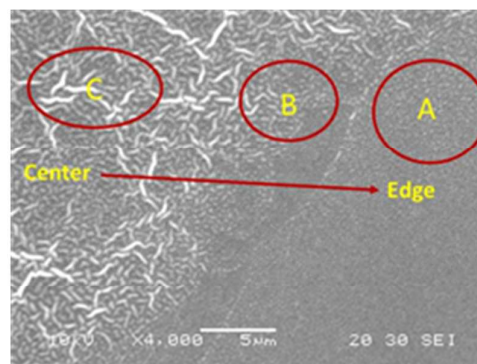


**Figure 3.** SEM image of spin coated **P1** (2mg/ml) film.

It was noteworthy that heterogeneous surface was observed. At area A, distinctly spherical micelles were formed, and at area B, the spherical micelle started to aggregate and elongate into ellipse shape. In comparison, wrinkle like dense polymer coating was observed at area C. The difference in morphologies could be resulted from the polymer surface concentration variance during the spin coating process as concentration at area A, which is close to the sample edge, is lower than that at area C, which is close to the sample center.

Instead of inhomogeneous surface as obtained in a diluted solution, high concentrations of dispersions were casted and the formed dense polymer coatings are shown in Figure 4. For polymers **P1** to **P4**, the polymer coatings showed a wrinkle-like continuous surface (Figure 4a-d). For **P5**, it exhibited a segregated morphology, which was different from the rest of polymers and is possibly due to the poor solubility of the polymer in the casting solvent (chloroform). As **P5** has very poor solubility in chloroform, the polymer would aggregate during the casting process and hence only separated patches were observed on the Si surface after solvent evaporation

(Figure 4e). In a control experiment, neat PEG polymer exhibited a homogeneous and amorphous film (Figure 4f).

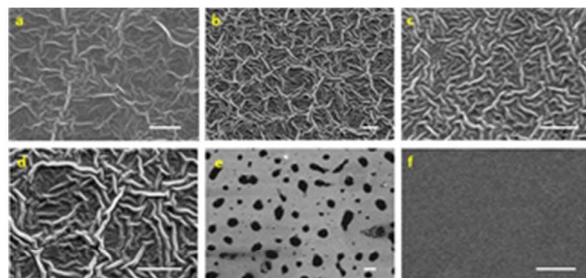
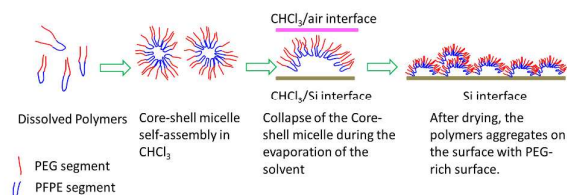


**Figure 4.** SEM images of (a) P1; (b) P2; (c) P3; (d) P4; (e) P5; and (f) neat PEG thin film morphology. Scale bar: 10  $\mu\text{m}$

When the block copolymer solution spin-coated with high concentration dispersion (solid content at 15 mg/ml), a continuous wrinkle like polymer coating was formed (with diameter around 800 – 1000 nm and aspect ratio around 8-10). For polymers with good solubility in chloroform (P1-P4), the attributes of the polymers, such as the molecular weight and the length of amphiphilic segments, have minor influence on the final morphology and no significant variation of the wrinkle width for P1-P4 was observed. Wrinkle-like morphologies are interesting features for block copolymers and are promising in a wide range of applications.<sup>61-65</sup> The occurrence of such morphology would originate was attributed to the balance between the isotropic coalescence and the anisotropic self-assembly of core/shell (micelle) particles. With the fast evaporation of solvent, the block copolymer micelles were concentrated. The aggregation of the micelles happened. The shell layer of PEG block from different micelles would collapse and coalesce to larger particles. This process would lead to entropy reduction due to the increasing overlap volume between the molecular chains on micelle shell layer. Thus, in order to depress the contribution of entropic reduction due to the collapse and coalescence of PEG shell, the micelles tended to anisotropically assemble and formed the wrinkle like structure.<sup>61, 66</sup> The self-assembly process is illustrated by a cartoon as shown in Scheme 2.



**Scheme 2.** Illustrative description on the self-assembly process of the triblock copolymers (P3 as example).

PEG and PFPE segments are mutually incompatible due to their different hydrophobicity. The surface topography and phase image of the casting films in sub-micrometer scale were investigated using tapping mode atomic force microscopy (AFM) (Figure 5). In P1-P4, height images (Figure 5a, 5c, 5e, 5g), wrinkle-like structures were

observed which was consistent with the SEM results. In phase images, phase contrast appeared to be homogenous. It is possible that the formation of these wrinkle patterns is due to the self-organization of PEG-PFPE chains at the  $\text{CHCl}_3$ /air interface during spin coating process. The hydrophilic PEG segments tended to migrate into air/ $\text{CHCl}_3$  surface. The PFPE segments tended to embed into the bulk layer. These results further proved that the balance between the isotropic coalescence and anisotropic self-assembly resulted in PEG enrichment wrinkle like film surface.

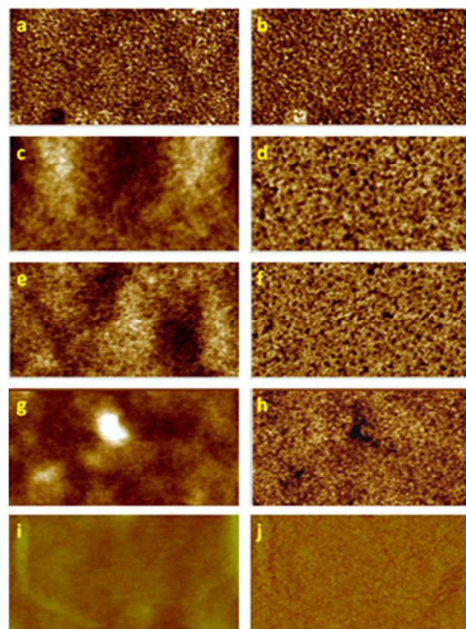


**Figure 5.** AFM images of triblock copolymer film. a) P1 height; b) P1 phase; c) P2 height; d) P2 phase; e) P3 height; f) P3 phase; g) P4 height; h) P4 phase; i) PEG height; and j) PEG phase; Scan size: 0.5  $\mu\text{m}$   $\times$  1  $\mu\text{m}$ .

#### Surface energy study

The PEG chains presumably grant some flexibility in the block copolymer. In a high humidity environment, (humidity around 70%), to minimize the enthalpy, the hydrophobic PFPE segments are preferably buried under the PEG groups. Thus the PEG segments show a substantial preference for enrichment at the air interface. In order to ascertain the orientation of the hydrophobic (PFPE) and hydrophilic (PEG) fragments on the substrate surface, static water contact angle analysis was performed. Surfaces for static water contact angle analysis were prepared on silicon wafers by spin coating 15% (w/v) solution of triblock copolymer in chloroform at 2000 rpm for 30 s. The results are summarized in Figure 6 and Table 4. It is interesting that all five polymers, given different length of PEG and PFPE fragments, exhibited hydrophilic nature on Si surface. For P1-P4, all water contact angles were less than 15°. For P5 with the highest fluorine content, the water contact angle is only about 58° whereas neat PFPE film typically gives water contact angle > 110°.<sup>67</sup> During the self-assembly process, the hydrophobic PFPE fragments of the triblock copolymer serve as the core of the micelle in chloroform solution<sup>53</sup> and during the micelle aggregation process

they have a much higher tendency to stay close to the Si surface, with the hydrophilic PEG fragment exposed to solution. One driving

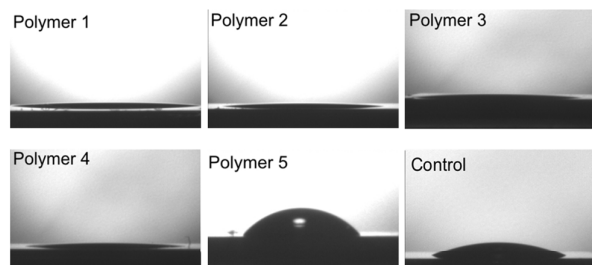


**Figure 6.** Water contact angle images of the polymers **P1-P5** and control Si substrate

**Table 4.** Summary of water contact angles of **P1-P5**.

Polymer	Contact Angle ( $^{\circ}$ )
<b>P1</b>	12.3 $\pm$ 1.7
<b>P2</b>	10.8 $\pm$ 1.2
<b>P3</b>	10.6 $\pm$ 1.5
<b>P4</b>	10.2 $\pm$ 2.1
<b>P5</b>	58.5 $\pm$ 4.3

force for such a kind of orientation would be the different solubility of the PFPE and PEG fragments in the casting solvent (chloroform). Since the PEG fragments are more soluble in chloroform compared with the PFPE fragments, the PEG blocks of the polymer have higher tendency to be surrounded by the solvent molecules and stay on the film/solution interface whereas the PFPE fragments will precipitate out and accumulate on the Si surface. For neat PEG film, the water contact angle was ca. 60°. Surprisingly for **P1-P4**, even though there were hydrophobic PFPE fragments present in the copolymer backbone, the contact angle was smaller than 15° for all four polymers, which is much smaller than that of pure PEG polymers. The wetting behaviour of these films was determined by film chemical composition as well as morphology. The increased hydrophilicity compared with PEG film would most likely originate from the wrinkle-like morphology of the self-assembled films. It is well known that for a given chemical composition, increasing the roughness would result in more hydrophobic or more hydrophilic surface depending on the wettability of the material in the smooth state. For hydrophilic PEG rich surface, the microstructure is readily immersed by water with no air entrapped. Thus the surface can accommodate the full volume of the water and is fully wetted (Wenzel-type roughness effect). For polymer **P5**, as it exhibited poor solubility in chloroform, the self-assembly process has limited effect on its morphology and the distribution of the PFPE and PEG fragments in the film is hence envisaged to be more random. As a result, the water contact angle is about 58°, which is higher than that of **P1-P4**, and the surface energy was lower due to higher concentration of fluorinated fragments on the surface.

#### Antibacterial study

PFPE and PEG polymers have been well investigated as antimicrobial and fouling-release coating materials. In this regard, the PFPE/PEG triblock copolymers are rather intriguing as potential antibacterial polymers due to the synergistic effect of the two components. Rather than the inclusion of biocidal components, the combination of environmentally benign materials, PFPE/PEG block copolymer is certainly regarded as a better choice. For fouling-release and antibacterial coating materials for domestic and biomedical applications, inhibition of the colonization of common pathogens, such as *E. coli* and *S. aureus*, is the key criteria to judge the effectiveness of the coating material. A qualitative analysis of the antimicrobial activities against *E. coli* and *S. aureus* of the prepared PFPE/PEG triblock copolymers was carried out on silicon surface. **P1-P3** thin films were spin coated onto the Si surface. The SEM images of the investigated surfaces are used to analyse the bacterial attachment. The quantitative analysis data are summarized in Figure 7. For *E. coli* on Si surfaces, all three polymers coating exhibited vivid antimicrobial properties with a very limited number of bacterial adhered on the coated substrates which clearly demonstrates the superior antimicrobial nature of this series of PFPE/PEG tri-block copolymers. After a settlement of 24 h, the percentage of attached bacterial ranged between 0% - 3% after coating with **P1-P3** on Si surface. For *S. aureus*, decreased bacterial attachments on **P1-P3** surfaces were observed as well. **P3** showed very good performance on prohibition of *S. aureus* attachment over **P1** and **P2**. This is because **P3** has high molecular weight as well as the longest PEG chain. For **P3**, the PEG segment has a MW of ca. 2000 g/mol whereas for **P1** and **P2**, the PEG segment is about half the length and only has a MW of ca. 1000 g/mol. The superior antibacterial performance of the triblock copolymer is hypothesized to result from the PEG rich surface. PEGylated surfaces have been well studied for their resistance to protein adsorption, hence inhibiting the adhesion and colonization of cells on the coated surfaces. Increasing the chain length of the hydrophilic PEG segments in **P1-P3**, was surmised to enhance the fouling resistance. These promising results indicate that combining PFPE and PEG together to prepare block copolymers would be a rational strategy to achieve high performance antibacterial coating materials.

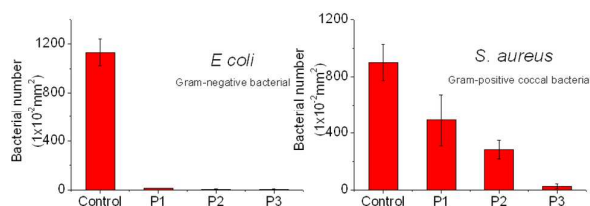


**Figure 7.** Average settlement of *E. coli* and *S. aureus* on coated polymer surface with Si substrates.

Given the understanding of PEG-based anti-fouling materials, the potential of swelling of such thin films due to their hydrophilicity would decrease the coating robustness for permanent sterile coating applications. Embedment of the hydrophobic PFTE component would resist water uptake and help improve the long-term applicability of the newly developed coating materials. This issue will be subject to further investigation to assess



the durability of these triblock copolymers as anti-bacterial coating materials.

## Conclusions

In summary, we have prepared a series of PFPE/PEG triblock copolymers (**P1-P5**) with controllable polymer geometry *via* thiol-ene click reaction in good yields. The self-assembly behavior of this group of newly developed amphiphilic polymers was investigated in detail by SEM and AFM. Polymers **P1-P4** were found to be soluble in organic solvents whereas **P5** was only soluble in fluorinated solvent. The self-assembled films of **P1-P4** on Si surface exhibited an intriguing wrinkle-like cross-linked morphology. The water contact angle and surface energy measurement indicated that the self-assembled films were more hydrophilic than neat PEG films, even though hydrophobic PFPE fragments were present in the copolymers. This was mainly due to the enrichment of the PEG fragments on the surface of the film and the specific orientation was envisaged due to the different solubility of the PEG and PFPE fragments in the casting solvent (chloroform). The antimicrobial properties of **P1-P3** were also investigated against *E. coli* and *S. aureus* on Si surfaces. Vivid antimicrobial properties of this series of copolymers were observed, indicating that the block copolymers of PFPE and PEG are potential high performance antimicrobial coating materials.

## Acknowledgements

The authors would like to acknowledge financial support (Grant No. 1123004023) from The Science and Engineering Research Council, Agency for Science, Technology and Research (A\*STAR), Singapore.

## Notes and references

1. P. Kingshott and H. J. Griesser, *Curr. Opin. Solid St. M.*, 1999, **4**, 403-412.
2. J. Genzer and K. Efimenko, *Biofouling*, 2006, **22**, 339-360.
3. S. Krishnan, C. J. Weinman and C. K. Ober, *J. Mater. Chem.*, 2008, **18**, 3405-3413.
4. C. M. Grozea and G. C. Walker, *Soft Matter*, 2009, **5**, 4088-4100.
5. A. Rosenhahn, S. Schilp, H. J. Kreuzer and M. Grunze, *Phys. Chem. Chem. Phys.*, 2010, **12**, 4275-4286.
6. M. Lejars, A. Margaiilan and C. Bressy, *Chem. Rev.*, 2012, **112**, 4347-4390.
7. R. F. Brady and I. L. Singer, *Biofouling*, 2000, **15**, 73-81.
8. M. Berglin, N. Lönn and P. Gatenholm, *Biofouling*, 2003, **19**, 63-69.
9. J. C. Yarbrough, J. P. Rolland, J. M. DeSimone, M. E. Callow, J. A. Finlay and J. A. Callow, *Macromolecules*, 2006, **39**, 2521-2528.
10. R. G. Chapman, E. Ostuni, S. Takayama, R. E. Holmlin, L. Yan and G. M. Whitesides, *J. Am. Chem. Soc.*, 2000, **122**, 8303-8304.
11. E. Ostuni, R. G. Chapman, R. E. Holmlin, S. Takayama and G. M. Whitesides, *Langmuir*, 2001, **17**, 5605-5620.
12. E. Ostuni, B. A. Grzybowski, M. Mrksich, C. S. Roberts and G. M. Whitesides, *Langmuir*, 2003, **19**, 1861-1872.
13. A. Statz, J. Finlay, J. Dalsin, M. Callow, J. A. Callow and P. B. Messersmith, *Biofouling*, 2006, **22**, 391-399.
14. T. Ekblad, G. Bergström, T. Ederth, S. L. Conlan, R. Mutton, A. S. Clare, S. Wang, Y. Liu, Q. Zhao, F. D'Souza, G. T. Donnelly, P. R. Willemsen, M. E. Pettitt, M. E. Callow, J. A. Callow and B. Liedberg, *Biomacromolecules*, 2008, **9**, 2775-2783.
15. P. Lundberg, A. Bruin, J. W. Klijnstra, A. M. Nystrom, M. Johansson, M. Malkoch and A. Hult, *ACS Appl. Mater. Interfaces*, 2010, **2**, 903-912.
16. D. J. Gan, A. Mueller and K. L. Wooley, *J. Polym. Sci. Part A Polym. Chem.*, 2003, **41**, 3531-3540.
17. C. S. Gudipati, C. M. Greenlief, J. A. Johnson, P. Prayongpan and K. L. Wooley, *J. Polym. Sci. Part A Polym. Chem.*, 2004, **42**, 6193-6208.
18. C. S. Gudipati, J. A. Finlay, J. A. Callow, M. E. Callow and K. L. Wooley, *Langmuir*, 2005, **21**, 3044-3053.
19. W. Du, Y. Li, A. M. Nyström, C. Cheng and K. L. Wooley, *J. Polym. Sci. Part A Polym. Chem.*, 2010, **48**, 3487-3496.
20. P. M. Imbesi, N. V. Gohad, M. J. Eller, B. Orihuela, D. Rittschof, E. A. Schweikert, A. S. Mount and K. L. Wooley, *Acc Nano*, 2012, **6**, 1503-1512.
21. P. M. Imbesi, C. Fidge, J. E. Raymond, S. I. Cauet and K. L. Wooley, *ACS Macro Lett.*, 2012, **1**, 473-477.
22. P. M. Imbesi, J. A. Finlay, N. Aldred, M. J. Eller, S. E. Felder, K. A. Pollack, A. T. Lonneck, J. E. Raymond, M. E. Mackay, E. A. Schweikert, A. S. Clare, J. A. Callow, M. E. Callow and K. L. Wooley, *Polym. Chem.*, 2012, **3**, 3121-3131.
23. J. P. Youngblood, L. Andruzzi, C. K. Ober, A. Hexemer, E. J. Kramer, J. A. Callow, J. A. Finlay and M. E. Callow, *Biofouling*, 2003, **19**, 91-98.
24. S. Krishnan, N. Wang, C. K. Ober, J. A. Finlay, M. E. Callow, J. A. Callow, A. Hexemer, K. E. Sohn, E. J. Kramer and D. A. Fischer, *Biomacromolecules*, 2006, **7**, 1449-1462.
25. S. Krishnan, R. Ayothi, A. Hexemer, J. A. Finlay, K. E. Sohn, R. Perry, C. K. Ober, E. J. Kramer, M. E. Callow, J. A. Callow and D. A. Fischer, *Langmuir*, 2006, **22**, 5075-5086.
26. C. J. Weinman, J. A. Finlay, D. Park, M. Y. Paik, S. Krishnan, H. S. Sundaram, M. Dimitriou, K. E. Sohn, M. E. Callow, J. A. Callow, D. L. Handlin, C. L. Willis, E. J. Kramer and C. K. Ober, *Langmuir*, 2009, **25**, 12266-12274.
27. D. Park, C. J. Weinman, J. A. Finlay, B. R. Fletcher, M. Y. Paik, H. S. Sundaram, M. D. Dimitriou, K. E. Sohn, M. E. Callow, J. A. Callow, D. L. Handlin, C. L. Willis, D. A. Fischer, E. J. Kramer and C. K. Ober, *Langmuir*, 2010, **26**, 9772-9781.
28. M. D. Dimitriou, Z. Zhou, H.-S. Yoo, K. L. Killips, J. A. Finlay, G. Cone, H. S. Sundaram, N. A. Lynd, K. P. Barteau, L. M. Campos, D. A. Fischer, M. E. Callow, J. A. Callow, C. K. Ober, C. J. Hawker and E. J. Kramer, *Langmuir*, 2011, **27**, 13762-13772.
29. C. K. Ober, S. Krishnan and Q. Lin, *Patent Number: US7709055 B2*, 2010.
30. C. K. Ober, S. Krishnan and Q. Lin, *Patent Number: US81922843 B2*, 2012.
31. C. K. Ober, C. J. Weinman, D. Park, D. L. Handlin and C. L. Willis, *Patent Number: EP20090718378*, 2011.
32. Z. Hu, L. Chen, D. E. Betts, A. Pandya, M. A. Hillmyer and J. M. DeSimone, *J. Am. Chem. Soc.*, 2008, **130**, 14244-14252.

33. Z. Hu, J. A. Finlay, L. Chen, D. E. Betts, M. A. Hillmyer, M. E. Callow, J. A. Callow and J. M. DeSimone, *Macromolecules*, 2009, **42**, 6999-7007.
34. Y. Wang, D. E. Betts, J. A. Finlay, L. Brewer, M. E. Callow, J. A. Callow, D. E. Wendt and J. M. DeSimone, *Macromolecules*, 2011, **44**, 878-885.
35. Y. Wang, J. A. Finlay, D. E. Betts, T. J. Merkel, J. C. Luft, M. E. Callow, J. A. Callow and J. M. DeSimone, *Langmuir*, 2011, **27**, 10365-10369.
36. Y. Wang, L. M. Pitet, J. A. Finlay, L. H. Brewer, G. Cone, D. E. Betts, M. E. Callow, J. A. Callow, D. E. Wendt, M. A. Hillmyer and J. M. DeSimone, *Biofouling*, 2011, **27**, 1139-1150.
37. R. K. Iha, K. L. Wooley, A. M. Nystrom, D. J. Burke, M. J. Kade and C. J. Hawker, *Chem. Rev.*, 2009, **109**, 5620-5686.
38. F. Dénès, M. Pichowicz, G. Povie and P. Renaud, *Chem. Rev.*, 2014, **114**, 2587-2693.
39. A. B. Lowe, *Polym. Chem.*, 2010, **1**, 17-36.
40. W. Xi, T. F. Scott, C. J. Kloxin and C. N. Bowman, *Adv. Funct. Mater.*, 2014, **24**, 2572-2590.
41. C. E. Hoyle and C. N. Bowman, *Angew. Chem. Int. Ed.*, 2010, **49**, 1540-1573.
42. V. Abetz, M. L. Arnal, V. Balsamso, C. Coenjarts, J. G. Gohy, M. A. Hillmyer, M. Li, A. J. Mueller and C. K. Ober, in *Block Copolymers II: Advances in Polymer Science*, ed. V. Abetz, Springer, Berlin, 2005.
43. Z. L. Tyrrell, Y. Shen and M. Radosz, *Prog. Polym. Sci.*, 2010, **35**, 1128-1143.
44. T. P. Lodge, K. J. Hanley, B. Pudil and V. Alahapperuma, *Macromolecules*, 2003, **36**, 816-822.
45. T. P. Lodge, B. Pudil and K. J. Hanley, *Macromolecules*, 2002, **35**, 4707-4717.
46. I. Park, B. Lee, J. Ryu, K. Im, J. Yoon, M. Ree and T. Chang, *Macromolecules*, 2005, **38**, 10532-10536.
47. S. Park, J.-Y. Wang, B. Kim, W. Chen and T. P. Russell, *Macromolecules*, 2007, **40**, 9059-9063.
48. H. Cui, Z. Chen, S. Zhong, K. L. Wooley and D. J. Pochan, *Science*, 2007, **317**, 647-650.
49. C. M. Grozea, N. Gunari, J. A. Finlay, D. Grozea, M. E. Callow, J. A. Callow, Z.-H. Lu and G. C. Walker, *Biomacromolecules*, 2009, **10**, 1004-1012.
50. C. Holtze, A. C. Rowat, J. J. Agresti, J. B. Hutchison, F. E. Angilè, C. H. J. Schmitz, S. Köster, H. Duan, K. J. Humphry, R. A. Scanga, J. S. Johnson, D. Pisignano and D. A. Weitz, *Lab Chip*, 2008, **8**, 1632-1639.
51. S. Köster, F. E. Angilè, H. Duan, J. J. Agresti, A. Wintner, C. Schmitz, A. C. Rowat, C. A. Merten, D. Pisignano, A. D. Griffiths and D. A. Weitz, *Lab Chip*, 2008, **8**, 1110-1115.
52. L. Mazutis and A. D. Griffiths, *Lab on a Chip*, 2012, **12**, 1800-1806.
53. I. Platzman, J.-W. Janiesch and J. P. Spatz, *J. Am. Chem. Soc.*, 2013, **135**, 3339-3342.
54. C. J. Vanoss, L. Ju, M. K. Chaudhury and R. J. Good, *J. Coll. Interface Sci.*, 1989, **128**, 313-319.
55. R. J. Good, M. K. Chaudhury and C. J. van Oss, ed. L. H. Lee, Plenum, New York, 1994.
56. X. Wang, Q. Ye, J. Song, C. M. Cho, C. He and J. Xu, *RSC Adv.*, 2015, **5**, 4547-4553.
57. S. M. Jain, X. B. Gong, L. E. Scriven and F. S. Bates, *Phys. Rev. Lett.*, 2006, **96**.
58. A. Blanazs, S. P. Armes and A. J. Ryan, *Macromol. Rapid Comm.*, 2009, **30**, 267-277.
59. R. Nagarajan and K. Ganesh, *J. Chem. Phys.*, 1989, **90**, 5843-5856.
60. J. Noolandi and K. M. Hong, *Macromolecules*, 1983, **16**, 1443-1448.
61. L. Guo, Y. Jiang, S. Chen, T. Qiu and X. Li, *Macromolecules*, 2014, **47**, 165-174.
62. S. H. Kang, J.-H. Na, S. N. Moon, W. I. Lee, P. J. Yoo and S.-D. Lee, *Langmuir*, 2012, **28**, 3576-3582.
63. W. Li, T. Tian, Y. Lan, W. Zhu, J. Li, M. Zhang, Y. Ju and G. Li, *Polym. Chem.*, 2014, **5**, 743-751.
64. E. Nehlig, R. Schneider, L. Vidal, G. Clavier and L. Balan, *Langmuir*, 2012, **28**, 17795-17802.
65. P. Samyn, M. P. Laborie, A. P. Mathew, A. Airoudj, H. Haidara and V. Roucoules, *Langmuir*, 2012, **28**, 1427-1438.
66. C. A. Dreiss, *Soft Matter*, 2007, **3**, 956-970.
67. Q. W. Yuan, ed. J. E. Mark, Oxford University Press, Oxford, UK, 1999.
68. J. M. Lagarón, M. J. Ocio and A. López-Rubio, eds. J. M. Lagarón, M. J. Ocio and A. López-Rubio, John Wiley & Sons, Inc Hoboken, NJ, USA., 2012.
69. F. C. Cebeci, Z. Z. Wu, L. Zhai, R. E. Cohen and M. F. Rubner, *Langmuir*, 2006, **22**, 2856-2862.
70. K. Liu, X. Yao and L. Jiang, *Chem. Soc. Rev.*, 2010, **39**, 3240-3255.
71. E. Martines, K. Seunarine, H. Morgan, N. Gadegaard, C. D. W. Wilkinson and M. O. Riehle, *Nano Lett.*, 2005, **5**, 2097-2103.
72. C. W. Extrand, S. I. Moon, P. Hall and D. Schmidt, *Langmuir*, 2007, **23**, 8882-8890.
73. R. N. Wenzel, *Ind. Eng. Chem.*, 1936, **28**, 988-994.
74. J. Bico, U. Thiele and D. Quere, *Colloid Surf. A*, 2002, **206**, 41-46.
75. N. Satyanarayana and S. K. Sinha, *J. Phys. D: Appl. Phys.*, 2005, **38**, 3512-3522.

## Graphical Abstract

### Perfluoropolyether/poly(ethylene glycol) triblock copolymers with controllable self-assembly behaviour for highly efficient anti-bacterial materials

Jing Song,<sup>†</sup> Qun Ye,<sup>†</sup> Wang Ting Lee,<sup>‡</sup> Xiaobai Wang,<sup>†</sup> Tao He,<sup>†</sup> Kwok Wei Shah,<sup>†</sup> Jianwei

Xu<sup>\*,†,‡</sup>

<sup>†</sup> Institute of Materials Research and Engineering, A\*STAR (Agency for Science, Technology and Research), 3 Research Link, Singapore 117602

<sup>‡</sup> Department of Chemistry, National University of Singapore, 3 Science Drive 3, Singapore 117543

[jw-xu@imre.a-star.edu.sg](mailto:jw-xu@imre.a-star.edu.sg)

